Anisotropic metal deposition on TiO2 particles by electric-field-induced charge separation

Supakit Tiewcharoen, Chompunuch Warakulwit, Veronique Lapeyre, Patrick Garrigue, Lucas Fourier, Catherine Elissalde, Sonia Buffière, Philippe Legros, Marion Gayot, Jumras Limtrakul, et al.

HAL Id: hal-01587892

https://hal.archives-ouvertes.fr/hal-01587892

Submitted on 25 Feb 2021

Anisotropic metal deposition on TiO$_2$ particles by electric-field-induced charge separation.

S. Tiewcharoen[a,b], C. Warakulwit[b], V. Lapeyre[a], P. Garrigue[a], L. Fourier[c], C. Elissalde[c], S. Buffiere[c], P. Legros[c], M. Gayot[c], J. Limtrakul[d] and A. Kuhn[a] *

a) Univ. Bordeaux, CNRS UMR 5255, Bordeaux INP, ENSCBP, 16 Avenue Pey Berland, 33607 Pessac, France

b) Department of Chemistry, Faculty of Science, Kasetsart University, 50 Ngam Wong Wan Rd, Lat Yao, Chatuchak, Bangkok, 10900, Thailand

c) CNRS, Univ. Bordeaux, ICMCB, UPR 9048, F-33600 Pessac, France

d) Department of Materials Science and Engineering, Vidyasirimedhi Institute of Science and Technology, Rayong 21210, Thailand

Supporting Information Placeholder

ABSTRACT: Deposition of metals on TiO$_2$ semiconductors (M-TiO$_2$) results in hybrid materials combining the interesting properties of both materials in a single Janus particle. Out of the large number of techniques that have been proposed to generate Janus particles, one of them is bipolar electrochemistry. This concept can be employed in a straightforward way for the site selective modification of conducting particles. However, it is much less obvious to apply to semiconductors. In this work we report the successful bulk synthesis of asymmetric isotropic M-TiO$_2$ particles based on the synergy of bipolar electrochemistry and photochemistry, thus overcoming important intrinsic limitations when they are used separately. We were able to break the symmetry of micro- and nanoparticles suspended in an electrolyte by modifying selectively and in a wireless way one side with either gold or platinum. Hybrid materials synthesized in this way are a first step towards high performance catalyst particles for example for photosplitting of water.

An efficient use of sun light as the primary and inexhaustible energy source is an essential precondition for the replacement of fossil fuels. Photocatalysis[1,2] is one of the many ways to benefit from solar energy, e.g. to produce chemicals. Several types of semiconductors, including TiO$_2$, ZnO, CdS, Fe$_2$O$_3$, MoO$_3$, etc. are frequently applied as photocatalysts since they have band gaps suitable for harvesting sun light.[3-7] Titaniumdioxide (TiO$_2$) is the most famous of these candidates and its properties include furthermore non-toxicity, high stability and efficiency.

Photocatalysts absorb solar energy quanta with energies larger than the band gap and generate electron-hole pairs (e$^-$-h$^+$); electrons in the valence band are excited to the conduction band, leaving holes behind. The electrons and holes then migrate to the surface to react with chemical species in order to form products. The major drawback of semiconductor materials is usually charge carrier recombination. Furthermore, the band gap of some semiconductors such as TiO$_2$ has limitations with respect to the utilization of visible light, thus reducing the overall quantum efficiency.[3,7-9]

Metal-TiO$_2$ semiconductor (M-TiO$_2$) hybrids combine the properties of two materials in one, a good strategy to solve such problems. The deposition of plasmonic metals with high work functions, such as Au, Pt, Pd, etc., on a semiconductor enhances the efficiency of charge separation because these metals act as an electron sink to overcome the Schottky barrier at the metal-semiconductor interface and also enhance light absorption in the visible region.[10-12] For example, the modification of TiO$_2$ with gold improves the charge separation in TiO$_2$ by promoting under irradiation the transfer of the generated electrons from the semiconductor to the gold nanoparticles because the Fermi level of gold shifts close to the Fermi level of the semiconductor.[13] Many reports studying the deposition of different metals on TiO$_2$ with various methods have shown that the catalytic activity of hybrid materials is much higher compared to an unmodified semiconductor.[14-17] In addition, the morphology of the deposited materials is gaining importance in engineering as it affects the surface plasmon resonance (SPR) properties, the optical absorption and the generation of electron-hole pairs for photocatalysis.[18]

In this context so-called Janus particles[19,20] are outstanding candidates as multi-functional catalysts, since their surfaces have two or more distinct physico-chemical properties. M-TiO$_2$ Janus objects in particular are very promising and interesting materials because the junction which combines the metal and the dielectric oxide can generate strong local electric near-fields.[18] For this reason, many literature examples demonstrated a high catalytic activity of M-TiO$_2$ Janus particles with respect to various reactions.[18,21,22] Seh et al found that the photocatalytic hydrogen generation on Janus Au-TiO$_2$ materials is much more efficient due to the stronger localization of the plasmonic near-field close to the Au-TiO$_2$ interface at one side of the particles.[18,23]

M-TiO$_2$ Janus particles can be synthesized by several methods.[18,21,24,25] Bipolar electrodeposition, based on the polarization of conducting objects in electric fields is often used to break the symmetry, and in this way generates asymmetric objects.[26-31] This low-cost and easy to set up approach allows the bulk synthesis of Janus particles[32-35] However, this strategy cannot be applied directly to the deposition of metal on semiconductor materials due to their low conductivity. Therefore, an additional light source is required to activate the formation of charge carriers inside the semiconductor. Based on this concept, Ongaro et al[22] reported for the first time a site selective deposition of gold on TiO$_2$ nanofibers as anisotropic substrates, using UV light and a strong external electric field. The authors assumed that the redox reactions occurred by activation with incident light, while the electric field enhances charge separation, leading to electric field assisted photochemistry.

In this work, we report on two major advances with respect to the controlled bipolar modification of semiconductor particles:

-the successful modification of isotropic TiO$_2$ semiconductor objects by light-induced bipolar electrochemistry. Compared to anisotropic objects, such as tubes, rods or fibers, which orient parallel to the electric field upon polarization[36], this is much more challenging because they can rotate during the deposition process, thus preventing the generation of well-defined Janus particles.

-the modification of nanosized objects, which is usually not possible with bipolar electrochemistry. This is due to the fact that in classic bipolar electrochemistry the electric field which needs to be applied is indirectly proportional to the characteristic size of the object, meaning that nanoparticles usually require fields in the range of MV/m. Investigating the mechanism of metal deposition on TiO_2, we were able to demonstrate that it is possible to achieve metal deposition with electric fields three orders of magnitude lower than the ones required by the concept of classic bipolar electrochemistry. Consequently, even particles in the 10nm range can be for the first time selectively modified due to the synergetic combination of electric field and light. The so-obtained Janus objects might be used for a wide variety of applications such as hydrogen and oxygen evolution[37–39] as well as the catalytic degradation of organic compounds[13,24].

Experimental Section

Chemicals

Gold(III) chloride trihydrate (>99.9%, $HAuCl_4.3H_2O$), hexachloroplatinic acid hydrate (>99.9%, $H_2PtCl_6.xH_2O$), absolute ethanol, ammonium chloride (99.99% NH_4Cl), agarose (low gelling temperature), TiO_2 powder (rutile-type structure- 99.5% purity - average particle size of 100 nm) and nanoparticles based on a titanium(IV)oxide mixture of rutile and anatase (< 150 nm, dispersion 33-37%wt in water) were purchased from Sigma Aldrich. Titanium(IV) oxide, anatase (TiO_2, 99.6%, 3-6 mm sintered pieces), was purchased from Alfa Aesar. The metal deposition solution was prepared in a 95:5%V mixture of milliQ water (resistivity =18 MΩ cm) and absolute ethanol (abs EtOH) .

Materials and Cells

A DC high power supply, Heinzinger, PNC 10000-200POS, was used for this work. The light source was a LC8, HAMAMATSU, 200W mercury–xenon lamp (irradiation between 300 and 450 nm, UV). Reactions were performed by using two kinds of cells. Cell1: Home-made glass cell composed of three-compartments, open on the upper side to allow UV irradiation. The central chamber, in which the substrates and the reagents are located, is separated from the two electrode compartments by a glass septum (thickness 2 mm, porosity G2). The feeder electrodes in the cathodic and anodic compartment are a gold plate and a platinum wire, respectively. Cell2: Home-made plastic-glass cell without membranes, the distance between the two feeder electrodes is 3cm. The reaction compartment volume is about 1mL. The feeder electrodes are graphite plates.

Instruments

Scanning Electron Microscopy (SEM) images were obtained with a Hitachi Tabletop Microscope TM-1000. High Resolution Scanning Electron Microscopy (HRSEM) investigations were conducted using a JEOL 6700F. The TiO_2 nanoparticles were examined with a JEOL high-resolution transmission electron microscope (HRTEM). The samples were prepared by casting a drop of the particle suspension (~1 mg/mL) in water onto a 200-mesh carbon-coated copper grid. For determination of the chemical nature of the deposited elements, Energy Dispersive X-ray Spectroscopy (EDX) has been used (JEOL detector Si-Li).

Bipolar deposition of metal nanoparticles (M = Au and Pt) on macroscopic TiO_2 objects (macro-TiO_2)

Rather big TiO_2 objects (macro-TiO_2) (Anatase, ~3-6 mm sintered pieces) particles were placed in a 2 mM $HAuCl_4.3H_2O$ or 5 mM $H_2PtCl_6.xH_2O$ solution in the reaction compartment, while the electrode compartments were filled with 1 mM NH_4Cl in abs EtOH.

Subsequently, three kinds of experiments were performed in cell1: 1) Application of an external electric field (3-33 kV/m) without UV irradiation; 2) Exposure to UV irradiation with varying intensity (5 -100 %) without an external electric field; 3) Combining UV irradiation and external electric field. These experiments were carried out for periods varying from 10 to 60s. After the reaction, the samples were washed with distilled water and ethanol, and dried at room temperature.

Synthesis of TiO_2 microsphere (micro-TiO_2)

TiO_2 micro-spheres were prepared by a spray-drying technique (B-290 Buchi® apparatus) from a suspension of TiO_2 powder (Rutile) in demineralised water. The solid loading of the suspension was fixed to 25wt% to ensure a correct formation of droplets and a homogeneous shaping of the final particles. The mixing of liquid feed with hot air within a nozzle initiates the drying stage through rapid evaporation of the solvent and formation of dense and regular spheres. The particles pass through a cyclone to be separated from the humid air and dry spherical granules are collected. The conditions such as inlet temperature, aspiration rate, feed rate and gas flow were set at 220°C, 100%, 20% and 45ml/min respectively. The size of the as-obtained microspheres ranging from 10 up to 65 μm was determined by SEM analysis.

Deposition of metal nanoparticles (M = Au and Pt) on TiO_2 microspheres (M/micro-TiO_2) and nanoparticles (M/nano-TiO_2)

micro-TiO_2 or nano-TiO_2 powder was dispersed in a mixture of agarose gel (1.4%w/v in milliQ water) containing 2 mM $HAuCl_4.3H_2O$ or 5 mM $H_2PtCl_6.xH_2O$ in the reaction compartment (0.05% w/v), while the electrode compartments were filled with a mixture of agarose gel and 1 mM NH_4Cl in abs EtOH. Subsequently, the three types of experiments were performed in cell2 analogue to the experiments with macro-TiO_2.

Results and Discussion

1. Deposition of metal nanoparticles (M = Au and Pt) on macro-TiO_2 objects

When a semiconductor object absorbs light with an energy greater than its band gap energy (E_g), electrons in the valence band (VB) are promoted to the conduction band (CB), leaving holes behind. Then e^- and h^+ are migrating to the surface of the object and can locally trigger redox reactions if the object is in a solution containing active redox species. However if at the same time a strong electric field is applied to this solution it leads to a positive (δ^+) and negative (δ^-) polarization at the extremities of the semiconductor object (Figure 1). The external strong electric field and the induced polarization effect result in band bending and lead to an internal electric field which facilitates the separation of the charge carriers (e^--h^+ pairs) and their transport to opposite sides of the particle, where then reduction and oxidation reactions occur (Figure 1). This mechanism implies a remarkable difference when compared to normal bipolar electrodeposition on classic conductors. In the latter case the reduction occurs on the negatively polarized side of an object (the part facing the feeder anode), whereas for light induced bipolar deposition the reduction should occur on the positively polarized extremity of the semiconductor (the part facing the feeder cathode).

2
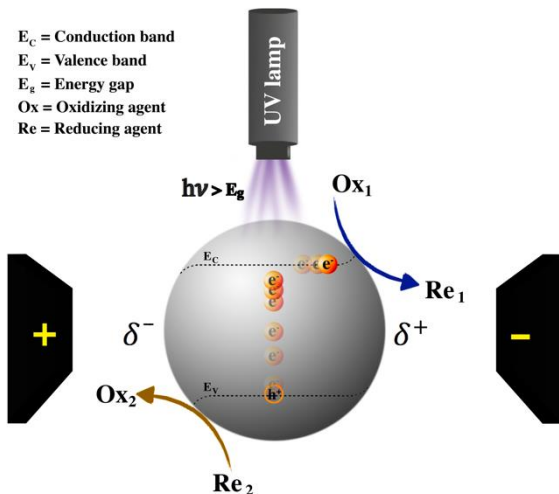
Figure 1. Schematic mechanism of metal deposition on TiO$_2$ particles.

In order to better understand and illustrate this mechanism of asymmetric reduction on semiconductor particles, we carried out a first experiment in which metal ions are reduced on macro-TiO$_2$ particles made out of anatase with dimensions in the millimetre range (about 3-6mm). For the first study, gold has been chosen as a deposit (Au/macro-TiO$_2$). The initial color of TiO$_2$ is completely white, but selectively turns into deep gray on the right or positive polarized side (δ^+) (Fig.2b) after applying an external electric field (E) of about 6kV/m and in the simultaneous presence of 100% UV light intensity for 60s reaction time in HAuCl$_4$.3H$_2$O media. This seems to indicate that gold particles are deposited on macro-TiO$_2$.
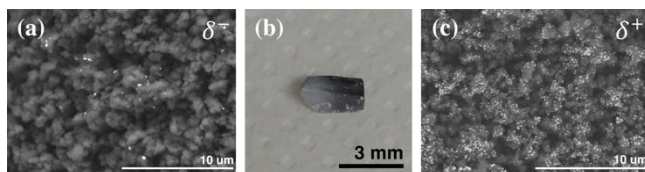

Figure 2. (a) SEM image revealing that only very few gold particles are deposited on the negatively polarized side, (b) Optical microscopy of the whole macro-TiO$_2$ object, and (c) SEM of the positively polarized side showing a high density of gold particles (white spots).

In order to confirm the asymmetric deposition, SEM images were recorded at both sides of the object (Fig.2a and c). The amount of gold particles at the δ^+ side is much higher than on the δ^- part which is indeed opposite of what would be obtained for conventional bipolar electrochemical deposition on conducting objects.[19,40]

Furthermore, when depositing platinum instead of gold in a second series of experiments an identical result is obtained. Platinum is exclusively observed on the δ^+ side (Fig.3a-c) at an electric field of 15kV/m with 50% UV intensity and 90s reaction time. In order to verify that the deposition is due to a synergistic effect of light and electric field, control experiments were performed by applying only an external electric field or exposing the particle only to UV light. Without light, the color of TiO$_2$ in Fig.3e does not change and the
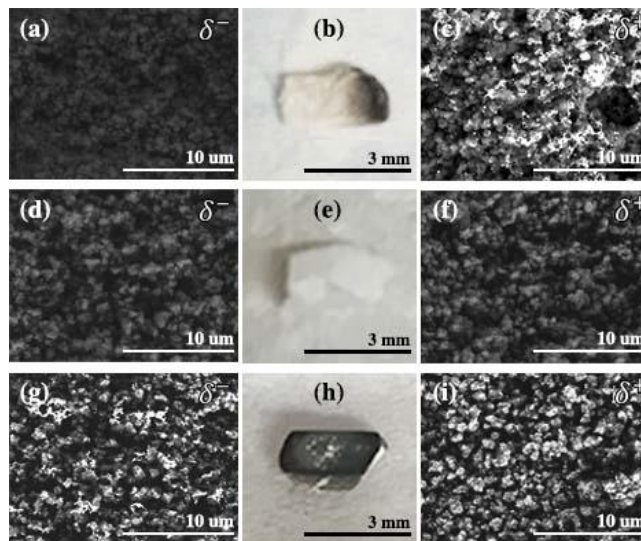

Figure 3. Deposition of platinum on macro-TiO$_2$ particles. (a-c) For simultaneous application of an electric field (E) and UV light, SEM images show no platinum on the δ^- side and platinum particles (white spots) on the δ^+ side; (d-f) No metal deposition is observed when only an electric field is applied; (g-i) Non-specific metal deposition is obtained when only UV light is used but no electric field.

2. Deposition of metal nanoparticles (M = Au and Pt) on micro-TiO$_2$

These first encouraging results obtained on macro-particles have led us to validate the process while addressing two main challenging issues: the downscaling of the particle size and the use of isotropic particles.
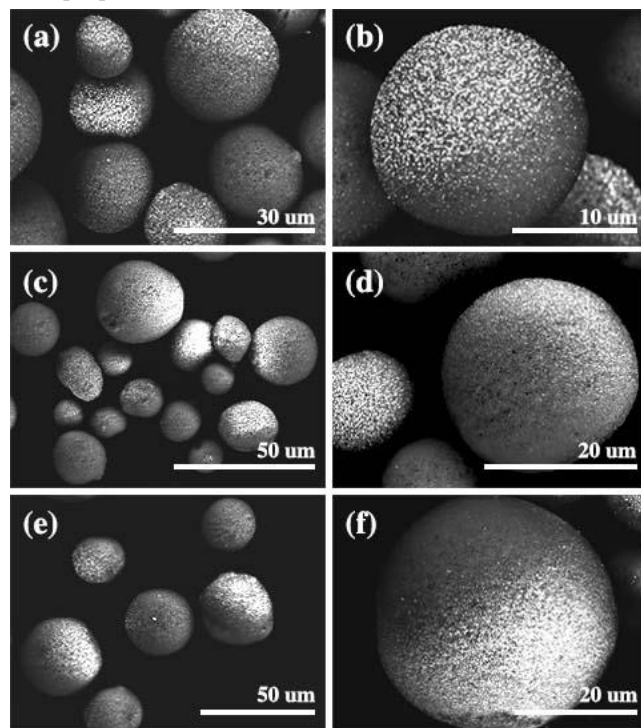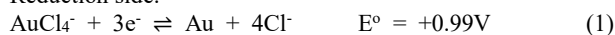
Figure 4. Asymmetric gold deposited on micro-TiO₂ obtained for simultaneous exposure for 30s to 20% UV light intensity and an electric field of (a-b) 33kV/m (c-d) 17kV/m and (e-f) 3kV/m.

Therefore, TiO₂ microspheres (micro-TiO₂) were then modified based on the same strategy. The asymmetric gold deposition on micro-TiO₂ was achieved by exposure to an external electric field of 33 kV/m and 20% UV light intensity for 30s (Fig.4a-b). Even when the electric field is reduced to 17 and 3 kV/m, the deposition still results in asymmetric particles (Fig.4c-d and e-f respectively). In order to confirm the chemical nature of the deposits elemental analysis of gold (Au) and titanium (Ti) was performed by energy dispersive X-ray spectroscopy (EDX) (Fig.5).

It is interesting to note that asymmetric gold deposition in a conventional bipolar electrochemical process with conductive objects of comparable diameter (>10μm) requires theoretically electric fields >24 kV/m for triggering the chemical reactions (1) and (2).[33] In the present series of experiments we could achieve electrodeposition even with an electric field as low as 3kV/m, that means almost one order of magnitude lower than the theoretical value needed for classic bipolar electrodeposition.

Reduction side:
$$AuCl_4^- + 3e^- \rightleftharpoons Au + 4Cl^- \qquad E^o = +0.99V \qquad (1)$$
Oxidation side:
$$2H_2O \rightleftharpoons O_2(g) + 4H^+ + 4e^- \qquad E^o = +1.23V \qquad (2)$$

This is due to the fact that in the present case, and in contrast to normal bipolar electrochemistry, it is not the electric field which generates the chemical driving force, but the light induced separation of charges provides the chemical energy. The electric field has only a secondary function, namely establishing an internal electric field inside the particle and thus dragging the charges towards the opposite extremities of the microparticles. Therefore, even an electric field strength which is far below the one theoretically required for inducing a bipolar electrochemical reaction will have a significant impact on the symmetry of the synthesized particles (see Figure 5).

The results in Figure 6 obtained by replacing the gold salt by a platinum salt confirm the pronounced asymmetric deposition of the metal even for 3kV/m, which should not lead to bipolar electrodeposition with normal electric conductors. This is very encouraging and allows speculating whether similar experiments can be carried out with nanoobjects instead of microobjects.
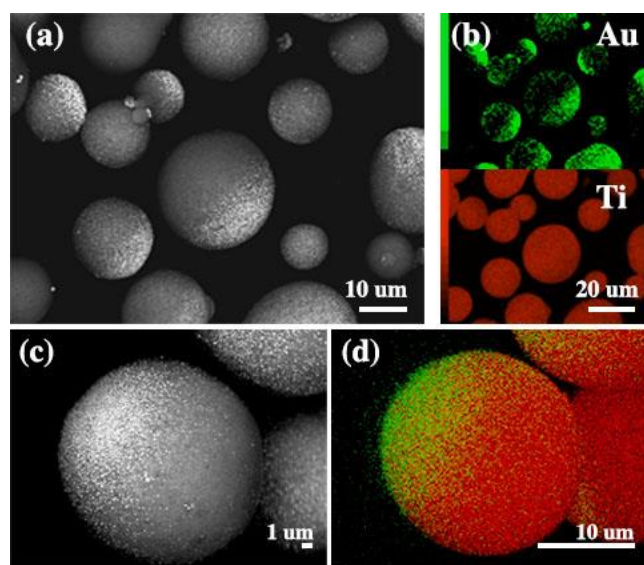
Figure 5. (a) and (c) SEM images of gold deposited on micro-TiO₂ by a simultaneous exposure for 30s to 20% UV light intensity and an electric field of 3kV/m. (b) and (d) EDX analysis of (a) and (c) respectively, red colour for Ti and green for Au.
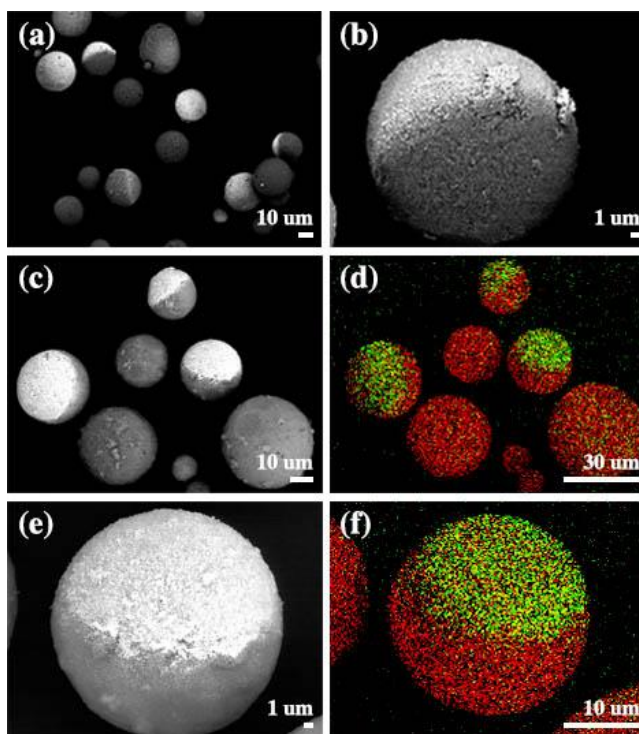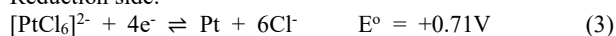

Figure 6. (a-c) and (e) SEM images of platinum deposited asymmetrically on micro-TiO₂ by a simultaneous exposure for 90s to 50% UV light intensity and an electric field of 3kV/m in a solution containing 5 mM H₂PtCl₆.xH₂O; (d) and (f) EDX analysis of (c) and (e) respectively, red colour for Ti and green for Pt.

Normal bipolar electrochemistry encounters severe limitations when experiments need to be carried out with very small objects because the driving voltage that has to be applied between the feeder electrodes scales inversely with the object size[40]. According to what has been observed with the above microparticles (Figures 4-6) this seems not to be the case for semiconductors because the electric field is not the driving force, but is just spatially directing the redox chemistry. Therefore, experiments with TiO₂ nanoparticles were carried out in the following.

3. Deposition of metal nanoparticles (M = Pt) on nano-TiO₂

From the above discussion, it becomes clear that the synergy between electric field and light should allow modifying also TiO₂ nanoparticles (nano-TiO₂). It is worth noting that using normal bipolar electrochemical deposition, an electric field with an amplitude of more than 5 MV/m is theoretically needed for a 100nm size nanoparticle. The corresponding involved chemical reactions are described as follows:

Reduction side:
$$[PtCl_6]^{2-} + 4e^- \rightleftharpoons Pt + 6Cl^- \qquad E^o = +0.71V \qquad (3)$$
Oxidation side:
$$2H_2O \rightleftharpoons O_2(g) + 4H^+ + 4e^- \qquad E^o = +1.23V \qquad (4)$$

4

The difference of the standard potentials of the two involved redox couples in equation (3) and (4) is 0.52V and at least this polarization potential difference has to exist between the extremities of the object (100 nm). Taking into account that the distance between the two feeder electrodes is 3.3 cm in the present set-up, this implies a potential difference of over 170 kV that has to be applied, which is impossible from a practical point of view.

However, when using the concept of light induced bipolar electrochemistry things change completely, because the electric field does not need to provide the direct driving force for the two redox reactions. This allows breaking the symmetry of modification even with relatively low electric fields. Figure 7 nicely illustrates this aspect. When a suspension of nano-TiO_2 is exposed just to UV light in the presence of platinum salt, the generated electron-hole pairs trigger the redox reactions (3) and (4) in a completely unspecific way everywhere on the semiconductor surface. As a result, Pt clusters with a typical size of 2-4 nm are covering the entire surface of the nano-TiO_2 objects.
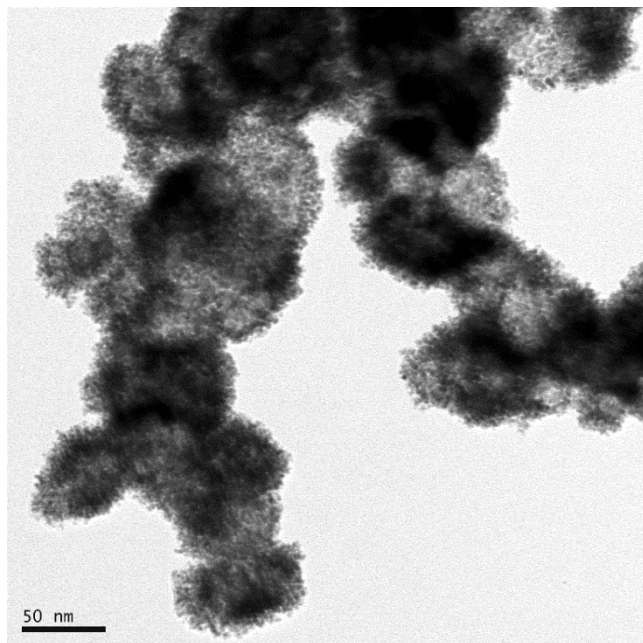
Figure 7. TEM image of nano-TiO_2 particles covered with platinum nanoclusters generated in an unspecific way by exposure for 90s to 50% UV light intensity.

However when applying simultaneously an electric field of 3kV/m, the situation drastically changes. The metal is no longer distributed homogeneously over the semiconductor particles, but rather undergoes single point electrodeposition, thus giving access for the first time to this kind of Janus nanoobjects (Fig. 8a). Statistically only one or very few platinum nanoclusters (black spots) are attached to one side of the nano-TiO_2, indicating that it is possible to break the deposition symmetry with electric fields that are more than three orders of magnitude lower compared to those required by classic bipolar electrochemistry. Figure 8b shows a HRTEM image of a typical junction between the metal and the semiconductor. Both of them exhibit crystalline order and seem to be well attached to each other.
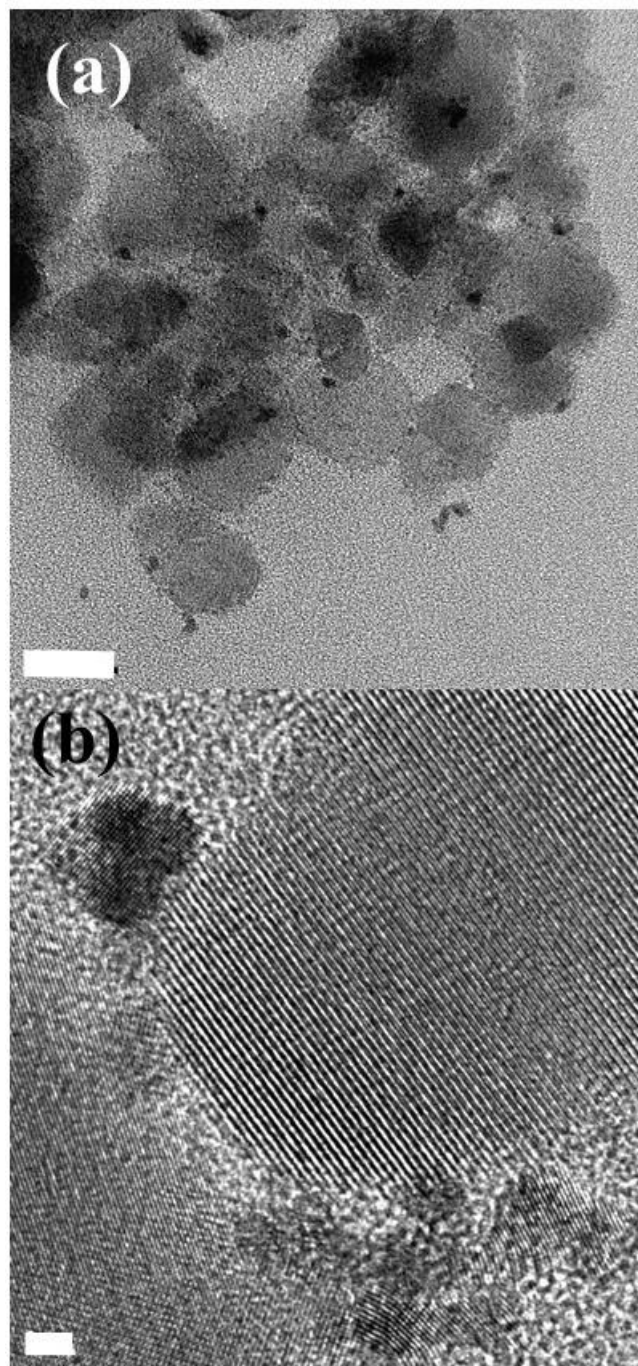
Figure 8. (a) TEM image of platinum nanoclusters generated in a selective way on nano-TiO_2 by exposure for 90s simultaneously to 50% UV light intensity and an electric field of 3kV/m. (b) HRTEM image for a typical deposit obtained under these conditions, zooming on the junction between the metal nanocluster and a nano-TiO_2 particle (scale bars are 20 and 2 nm respectively).

Conclusion

The concept of bipolar electrodeposition has been considerably extended by overcoming two major challenges:

- so far it was not possible to modify isotropic semi-conductor objects by bipolar electrodeposition of metals due to their rotation in the electric field during the modification step

- classic bipolar electrodeposition intrinsically requires very high electric fields for the modification of nanoobjects and therefore was so far mostly used for micron-sized particles

We could demonstrate that by taking advantage of the synergy between light and an electric field it is possible to induce bipolar behavior also on isotropic semiconductor particles suspended in a gel, and, most importantly, trigger metal deposition on particles with a characteristic size in the 10-30nm range. This only requires modest electric fields, which are over three orders of magnitude lower compared to what would be theoretically needed in a classic bipolar electrodeposition experiment without light.

Furthermore it has been possible to provide evidence that the deposition mechanism on semi-conducting particles is opposite to what has been observed for normal conductors, meaning that metal ion reduction occurs at the positively polarized pole of the object due to the electric field generated inside the semiconductor. The process is simple and low-cost and therefore can also be scaled up for industrial production. The so-obtained hybrid nanomaterials open the door for the synthesis of high-performance bifunctional catalysts for various applications, including water splitting and depollution of organic waste.

ACKNOWLEDGMENT

REFERENCES

(1) Natarajan, K.; Natarajan, T. S.; Kureshy, R. I.; Bajaj, H. C.; Jo, W. K.; Tayade, R. J. *Adv. Mater. Res.* **2015**, *1116*, 130–156.

(2) Ochiai, T.; Fujishima, A. *J. Photochem. Photobiol. C Photochem. Rev.* **2012**, *13* (4), 247–262.

(3) Nakata, K.; Fujishima, A. *J. Photochem. Photobiol. C Photochem. Rev.* **2012**, *13* (3), 169–189.

(4) Fujishima, A.; Zhang, X. *Comptes Rendus Chim.* **2006**, *9* (5–6), 750–760.

(5) Fujishima, A.; Rao, T. N.; Tryk, D. A. *J. Photochem. Photobiol. C Photochem. Rev.* **2000**, *1* (1), 1–21.

(6) Schneider, J.; Matsuoka, M.; Takeuchi, M.; Zhang, J.; Horiuchi, Y.; Anpo, M.; Bahnemann, D. W. *Chem. Rev.* **2014**, *114* (19), 9919–9986.

(7) Etacheri, V.; Di Valentin, C.; Schneider, J.; Bahnemann, D.; Pillai, S. C. *J. Photochem. Photobiol. C Photochem. Rev.* **2015**, *25*, 1–29.

(8) Thompson, T. L.; Yates, J. T. *Chem. Rev.* **2006**, *106* (10), 4428–4453.

(9) Sang, L.; Zhao, Y.; Burda, C. *Chem. Rev.* **2014**, *114* (19), 9283–9318.

(10) Gupta, B.; Melvin, A. A.; Matthews, T.; Dash, S.; Tyagi, A. K. *Renew. Sustain. Energy Rev.* **2016**, *58*, 1366–1375.

(11) Bumajdad, A.; Madkour, M. *Phys. Chem. Chem. Phys.* **2014**, *16* (16), 7146–7158.

(12) Jiang, R.; Li, B.; Fang, C.; Wang, J. *Adv. Mater.* **2014**, *26* (31), 5274–5309.

(13) *Comprehensive Nanoscience and Technology*; Academic Press, 2010.

(14) Zheng, Z.; Huang, B.; Qin, X.; Zhang, X.; Dai, Y.; Whangbo, M.-H. *J. Mater. Chem.* **2011**, *21* (25), 9079–9087.

(15) Ohyama, J.; Yamamoto, A.; Teramura, K.; Shishido, T.; Tanaka, T. *ACS Catal.* **2011**, *1* (3), 187–192.

(16) Zhang, Z.; Wang, Z.; Cao, S.-W.; Xue, C. *J. Phys. Chem. C* **2013**, *117* (49), 25939–25947.

(17) Pu, Y.-C.; Wang, G.; Chang, K.-D.; Ling, Y.; Lin, Y.-K.; Fitzmorris, B. C.; Liu, C.-M.; Lu, X.; Tong, Y.; Zhang, J. Z.; Hsu, Y.-J.; Li, Y. *Nano Lett.* **2013**, *13* (8), 3817–3823.

(18) Seh, Z. W.; Liu, S.; Low, M.; Zhang, S.-Y.; Liu, Z.; Mlayah, A.; Han, M.-Y. *Adv. Mater.* **2012**, *24* (17), 2310–2314.

(19) Loget, G.; Kuhn, A. *J. Mater. Chem.* **2012**, *22* (31), 15457–15474.

(20) Walther, A.; Müller, A. H. E. *Chem. Rev.* **2013**, *113* (7), 5194–5261.

(21) Dong, R.; Zhang, Q.; Gao, W.; Pei, A.; Ren, B. *ACS Nano* **2016**, *10* (1), 839–844.

(22) Ongaro, M.; Roche, J.; Kuhn, A.; Ugo, P. *ChemElectroChem* **2014**, *1* (12), 2048–2051.

(23) Pradhan, S.; Ghosh, D.; Chen, S. *ACS Appl. Mater. Interfaces* **2009**, *1* (9), 2060–2065.

(24) Fu, X.; Liu, J.; Yang, H.; Sun, J.; Li, X.; Zhang, X.; Jia, Y. *Mater. Chem. Phys.* **2011**, *130* (1–2), 334–339.

(25) Seh, Z. W.; Liu, S.; Zhang, S.-Y.; Bharathi, M. S.; Ramanarayan, H.; Low, M.; Shah, K. W.; Zhang, Y.-W.; Han, M.-Y. *Angew. Chem. Int. Ed.* **2011**, *50* (43), 10140–10143.

(26) Bradley, J.-C.; Chen, H.-M.; Crawford, J.; Eckert, J.; Ernazarova, K.; Kurzeja, T.; Lin, M.; McGee, M.; Nadler, W.; Stephens, S. G. *Nature* **1997**, *389*, 268–271.

(27) Ulrich, C.; Andersson, O.; Nyholm, L.; Björefors, F. *Angew. Chem. Int. Ed.* **2008**, *47* (16), 3034–3036.

(28) Inagi, S.; Ishiguro, Y.; Atobe, M.; Fuchigami, T. *Angew. Chem. Int. Ed.* **2010**, *49* (52), 10136–10139.

(29) Ramakrishnan, S.; Shannon, C. *Langmuir* **2010**, *26* (7), 4602–4606.

(30) Munktell, S.; Tydén, M.; Högström, J.; Nyholm, L.; Björefors, F. *Electrochem. Commun.* **2013**, *34*, 274–277.

(31) Loget, G.; So, S.; Hahn, R.; Schmuki, P. *J Mater Chem A* **2014**, *2* (42), 17740–17745.

(32) Warakulwit, C.; Nguyen, T.; Majimel, J.; Delville, M.-H.; Lapeyre, V.; Garrigue, P.; Ravaine, V.; Limtrakul, J.; Kuhn, A. *Nano Lett.* **2008**, *8* (2), 500–504.

(33) Loget, G.; Lapeyre, V.; Garrigue, P.; Warakulwit, C.; Limtrakul, J.; Delville, M.-H.; Kuhn, A. *Chem. Mater.* **2011**, *23* (10), 2595–2599.

(34) Loget, G.; Roche, J.; Gianessi, E.; Bouffier, L.; Kuhn, A. *J. Am. Chem. Soc.* **2012**, *134* (49), 20033–20036.

(35) Loget, G.; Roche, J.; Kuhn, A. *Adv. Mater.* **2012**, *24* (37), 5111–5116.

(36) Fattah, Z.; Garrigue, P.; Lapeyre, V.; Kuhn, A.; Bouffier, L. *J. Phys. Chem. C* **2012**, *116* (41), 22021–22027.

(37) Chen, S.; Thind, S. S.; Chen, A. *Electrochem. Commun.* **2016**, *63*, 10–17.

(38)   Walter, M. G.; Warren, E. L.; McKone, J. R.; Boettcher, S. W.; Mi, Q.; Santori, E. A.; Lewis, N. S. *Chem. Rev.* **2010**, *110* (11), 6446–6473.
(39)   Fujishima, A.; Honda, K. *Nature* **1972**, *238* (5358), 37–38.
(40)   Loget, G.; Zigah, D.; Bouffier, L.; Sojic, N.; Kuhn, A. *Acc. Chem. Res.* **2013**, *46* (11), 2513–2523.

TOC IMAGE